doi:10.1017/S1431927622009205

Charge Distribution Control with Atomic Resolution via Strain Engineering in Oxide Heterostructures

Yu-Mi Wu[1*], Y. Eren Suyolcu[2,1], Gideok Kim[1], Georg Christiani[1], Yi Wang[1], Bernhard Keimer[1], Gennady Logvenov[1], Peter A. van Aken[1]

[1.] Max Planck Institute for Solid State Research, Heisenbergstr.1, 70569 Stuttgart, Germany.
[2.] Department of Materials Science and Engineering, Cornell University, New York 14853, USA.

The exploration of strain engineering in complex oxide heterostructures has unveiled microscopic origins of macroscopic properties and has led to the precise control of the local physical behavior in materials at the nanoscale. Many studies in this field have focused on the coupling between manganites and cuprates [1]. However, due to the challenge of disentangling intrinsic and extrinsic effects at oxide interfaces, the role of the epitaxial strain for the charge transfer at the interface as well as the interfacial magnetic coupling in cuprate/manganite heterostructures is not yet well understood and explored. Here, we reveal the local charge distribution in manganite slabs by means of high-resolution electron microscopy and spectroscopy via investigating how the strain locally alters the electronic and magnetic properties of $La_2CuO_4/La_{0.5}Sr_{0.5}MnO_3/La_2CuO_4$ (LCO/LSMO/LCO) heterostructures, which were grown on three different substrates with different lattice spacings, $SrTiO_3$ (STO), $(LaAlO_3)_{0.3}$-$(Sr_2AlTaO_6)_{0.7}$ (LSAT) and $LaSrAlO_4$ (LSAO) [2].

The STEM-HAADF image and the elemental maps across the interfaces in Fig. 1 demonstrate a good macroscopic crystal quality with structurally coherent LCO/LSMO and LSMO/LCO interfaces. We observe differences in both the Mn distribution and the atomic stacking sequences at the top and bottom interfaces. The bottom LCO/LSMO interface has a stronger intermixing that spreads over ~1.5 nm, while the top LSMO/LCO interface is abrupt. Meanwhile, since the exchange interaction between Mn^{3+} and Mn^{4+} ions in manganites is at root of the correlation between conductivity and ferromagnetism, we focus on changes in the local Mn valence by probing the Mn $L_{2,3}$ edge fine structures, which reflect the unoccupied local Mn 3d density of states. The evolution of the Mn $L_{2,3}$ edge spectra on each atomic layer within LSMO of the trilayer on LSAT is shown in Fig. 2. We observe for all samples a significantly increased Mn valence near the bottom interface and a lowered Mn valence away from the interface. This indicates that the charge rearrangement results in two different magnetic phases: an interfacial ferromagnetically reduced layer and an enhanced ferromagnetic metallic region away from the interfaces. Furthermore, we find that the magnitude of the charge redistribution can be controlled via epitaxial strain, which further influences the macroscopic physical properties in a way opposed to strain effects reported on single-phase films. These results emphasize the importance of the interface effect, which here leads to a prominent charge redistribution away from the interface and alters its magnetic and electronic structure drastically [3].

References:

[1] Y. E. Suyolcu *et al.*, J. Supercond. Nov. Magn. **33** (2020), p. 107.
[2] Y.-M. Wu, Y. E. Suyolcu *et al.*, ACS Nano **15** (2021), p. 16228.

[3] This project has received funding from the European Union's Horizon 2020 research and innovation programme under grant agreement No. 823717 – ESTEEM3.

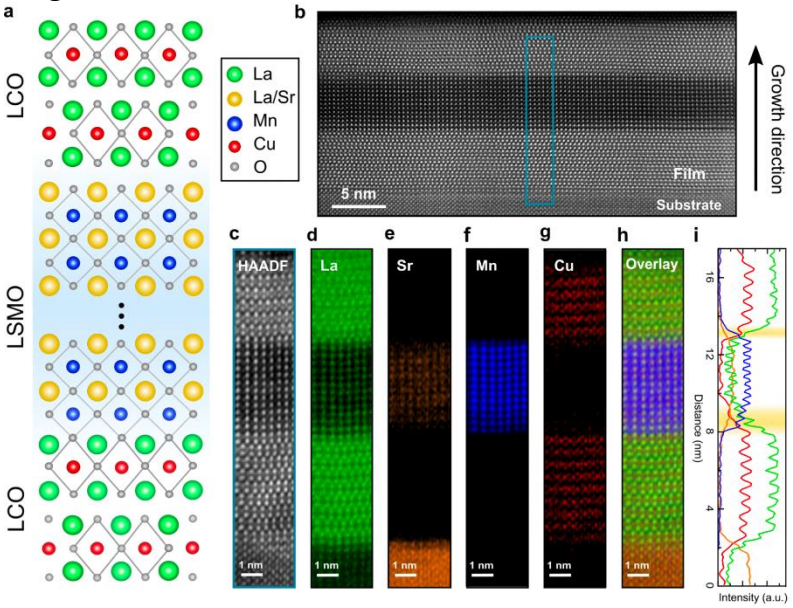

Figure 1. Overview of the LCO/LSMO/LCO interface lattice structure. (a) Schematic arrangement of atoms showing two different stacking sequences at two interfaces. (b) Low-magnetization STEM high-angle annular dark-field image of the film on LSAT (001). (c-h) Simultaneously-acquired ADF image and elemental concentration maps of La $M_{5,4}$, Sr $L_{3,2}$, Mn $L_{3,2}$, and Cu $L_{3,2}$ edges, respectively, and the overlay map from the area of the blue rectangle in (a). (i) Horizontally integrated intensity profiles of La (green), Sr (orange), Mn (blue), and Cu (red) distributions obtained from the maps.

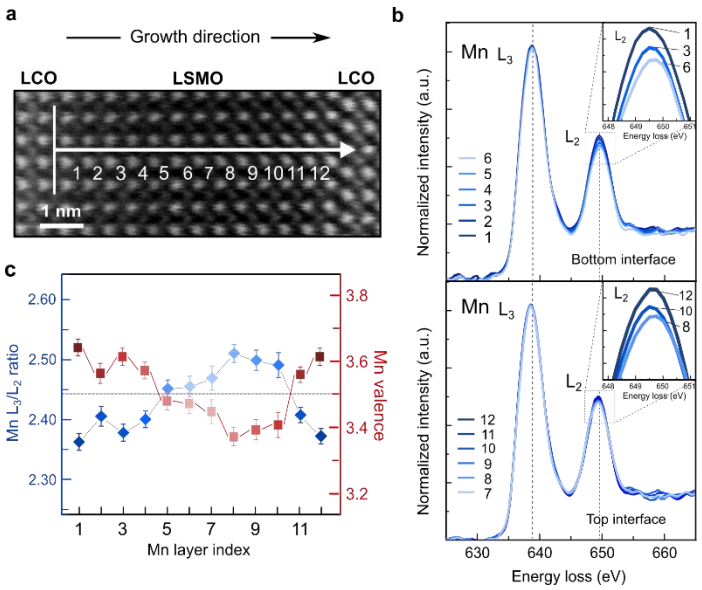

Figure 2. Electronic transition across the interfaces. (a) STEM-ADF image of LCO/LSMO/LCO film on LSAT. The white arrow indicates the region, where the EELS spectra were acquired. The vertical line

https://doi.org/10.1017/S1431927622009205 Published online by Cambridge University Press

indicates the averaging width while scanning. (b) Layer-resolved Mn $L_{3,2}$ edge spectra collected from the bottom interface into central LSMO, layers 1−6 in (a) and from central LSMO to the top interface, layers 7− 12 in (a). Zoomed views of the Mn L_2 white-line intensities are shown in the insets. (c) Local variation of in the Mn L_3/L_2 intensity ratio (blue) and the corresponding Mn valence (red) within LSMO.

https://doi.org/10.1017/S1431927622009205 Published online by Cambridge University Press